Effect of heating temperature and time on the phosphate adsorption capacity of thermally modified copper tailings

Runjuan Zhou, Youbao Wang, Ming Zhang, Jing Li, Yanan Gui, Yingying Tang, Beixin Yu and Yaru Yang

ABSTRACT

In the present study, copper tailings were treated at different temperatures (50–650 °C) and for various times (0.5–6 hours) and their phosphate adsorption capacity was investigated. The results showed that heating temperature significantly affected adsorption capacity. The highest capacity was observed in treatments at 310–350 °C. Heating time did not influence phosphate adsorption ability of copper tailings. Scanning electron microscopy, Barrett–Joyner–Halenda (BJH), and Fourier transform infrared spectroscopy (FTIR) were employed to characterize untreated copper tailings (raw CT) and copper tailings heated at 340 °C (CT340). The results showed that CT340 had a rougher surface, more and smaller pores, a larger surface area and higher FTIR transmittance than raw CT. These changes in texture might explain the increased phosphate adsorption of thermally modified copper tailings. Mathematical modeling showed that the Langmuir nonlinear model was the best fit to the current data. The maximum adsorption capacities of raw CT and CT340 were predicted as 2.08 mg/g and 14.25 mg/g at 298 K, pH 6.0, respectively.

Key words | adsorption, copper tailings, heating, modification, phosphate

Runjuan Zhou
Youbao Wang (corresponding author)
Jing Li
Yanan Gui
Yingying Tang
Beixin Yu
Yaru Yang
College of Life Sciences,
Anhui Normal University,
Wuhu, Anhui 241000,
China
E-mail: *wyb74@126.com*

Runjuan Zhou
Ming Zhang
College of Electrical Engineering,
Anhui Polytechnic University,
Wuhu, Anhui 241000,
China

INTRODUCTION

Water eutrophication facilitates algal growth and causes serious environmental and aesthetic problems (Kilpimaa *et al.* 2014). Discharge of phosphate from industrial and agricultural practices is one of the major factors causing water eutrophication. Hence, technologies for removing phosphate from water are in urgent demand (Wang *et al.* 2016a, 2016b).

Recently, numerous technologies have been developed to remove phosphate, such as physicochemical precipitation (Franco *et al.* 2017; Huang *et al.* 2017; Park *et al.* 2017), adsorption (Lv *et al.* 2013; Ashekuzzaman & Jiang 2014; Ren *et al.* 2015a, 2015b; Cui *et al.* 2016; Song *et al.* 2016; Jung *et al.* 2017; Koilraj & Sasaki 2017; Yang *et al.* 2018), ion exchange (Blaney *et al.* 2007; Zhang *et al.* 2017; Gan *et al.* 2018), membrane technology (Van Voorthuizen *et al.* 2005; Mouiya *et al.* 2018), and biological treatment (Debashan & Bashan 2004; Sevcenco *et al.* 2015). Among these methods, adsorption is the most promising because it has merits of low cost, simple operation, and potential regeneration (Jung *et al.* 2015; Park *et al.* 2015). Scientists have made many efforts to search for suitable adsorbents. Organic materials from municipal and agro-industrial wastes have been tried for phosphate removal (Bhatnagar & Sillanpää 2010). Inorganic adsorbents, such as steel slag (Barca *et al.* 2012; Claveau-Mallet *et al.* 2012; Yu *et al.* 2015; Wang *et al.* 2016a, 2016b), fly ash (Xu *et al.* 2010; Hermassi *et al.* 2017), red mud (Zhao *et al.* 2011; Yu *et al.* 2015; Ye *et al.* 2016), manganese, iron oxide and copper tailings (Zeng *et al.* 2004; Kong *et al.* 2008; Jiang *et al.* 2008; Zhang *et al.* 2010; Liu *et al.* 2012) have also been tested for phosphate removal. Tailings are by-products from mineral processing and generally contain high levels of heavy metals (e.g., Cu^{2+}, Zn^{2+}, Pb^{2+}, Mn^{2+}). Currently, tailings are landfilled directly, which is likely to pollute nearby environments.

Heavy metals can interact with inorganic anionic ligands (such as SO_4^{2-}, PO_4^{3-}, and SeO_4^{3-}) through precipitation, cooperative electrostatics and surface complexation (Awual *et al.* 2011; Dai *et al.* 2011; Liu *et al.* 2011; Zhang *et al.* 2011a, 2011b; Ren *et al.* 2015a, 2015b). These interactions not only remove phosphate from solution, but also immobilize heavy metals and reduce their availability to organisms,

doi: 10.2166/wst.2018.230

overall decreasing the harmful effects of both phosphate and heavy metals to environments (Khan & Jones 2009; Mignardi *et al.* 2012; Li *et al.* 2016b). In addition, tailings adsorbing phosphate are potential fertilizers, since similar methods have been applied to remove phosphate using fly ash and other wastes, and then developed as fertilizers (Debashan & Bashan 2004; Hermassi *et al.* 2017).

Cu^{2+} has a strong affinity with phosphate, and can adsorb phosphate effectively (Song *et al.* 2016). There have been several trials to evaluate phosphate adsorption capacity by copper tailings. The results showed effective adsorption of phosphate by copper tailings. The maximum adsorption capacity varied from 0.85 mg/g to 4.56 mg/g, depending on the source of materials and conditions (Kong *et al.* 2008; Zhang *et al.* 2010). The mixture of phosphate solution and copper tailings not only reduced the bioavailability of Cd, Cu, Pb, and Zn in sediments, but also minimized soil acidification and the potential risk of eutrophication caused by phosphate solution (Mignardi *et al.* 2012). These results highlight the potential to develop copper tailings as a phosphate adsorbent.

One factor affecting the phosphate adsorption ability of copper tailings was specific surface area (Jiang *et al.* 2008). Small and porous particles, especially nanostructured materials, showed better adsorption ability (Li *et al.* 2014). Thus, enlarging the specific surface area of copper tailings was a potential way to increase its phosphate adsorption ability. Treatment with heat cracked the surface and loosened the texture of steel slag, leading to better phosphate adsorption than untreated samples (Yu *et al.* 2015). To the best of our knowledge, whether thermal modification could improve the phosphate adsorption capacity of copper tailings has not been investigated. In the present study, the effects of heating temperature and heating time on the phosphate adsorption capacity of copper tailings were investigated. Next, the physical characteristics of thermally modified and unmodified copper tailings were compared. These results contribute to the future development of copper tailings as phosphate adsorbent and the understanding of the mechanisms of thermal modification underlying the improvement of phosphate adsorption of copper tailings.

MATERIALS AND METHODS

Materials

Copper tailings used in the present study were obtained from Tongling Copper Mines Plant, Anhui Province, China. All chemicals used were of analytical grade and purchased from Sinopharm Chemical Reagent Corporation. All solutions were prepared with ultrapure water. KH_2PO_4 was used to prepare the phosphate solution and the pH value was adjusted using NaOH or HCl solution.

Preparation of thermally modified copper tailings

Copper tailings were crushed and sieved using a 100-mesh net. Next, the copper tailings were placed in corundum crucibles and heated in a muffle furnace at 13 different temperatures (50, 100, 150, 200, 250, 300, 350, 400, 450, 500, 550, 600, and 650 °C), and six different heating time (0.5, 1, 2, 3, 4, 5, 6 hours). After naturally cooling to room temperature, the thermally modified copper tailings were stored in a desiccator.

Phosphate adsorption experiments

Copper tailings (1.5 g) were mixed with 100 mL of 50 mg/L phosphate solution in reaction vessels and the pH value was adjusted to 5.38 (equal to the pH of the 50 mg/L phosphate solution). Adsorption experiments were carried out at 25 ± 1 °C in shaker (150 rpm) for 3 hours. Next, samples were immediately filtered through a syringe filter (0.45 μm), and the residual phosphate content in solution was determined using the molybdenum blue spectrophotometric method (Wei & Qi 2009). Absorbance at 700 nm was determined using a UV-Vis spectrophotometer (U-3900, Hitachi). All experiments were repeated three times. The phosphate adsorption capacity of copper tailings q_t, (mg/g) at time t and equilibrium q_e (mg/g) were calculated using the following equations (Mitrogiannis *et al.* 2017):

$$q_t = (C_i - C_t)V/m$$

$$q_e = (C_i - C_e)V/m$$

where m (g) is mass of adsorbent, V (L) is volume of phosphate solution. C_i, C_t and C_e (mg/L) represents phosphate concentration in solution at the start, time t, and equilibrium, respectively.

Adsorption isotherm experiments

Two groups of samples were prepared: raw copper tailings (raw CT) and copper tailings heated at 340 °C for 2 hours (CT340). Phosphate solutions with concentrations ranging

from 0 to 300 mg/L (for raw CT) and from 0 to 500 mg/L (for CT340) were prepared. Phosphate adsorption isotherms were determined by adding 1.5 g of adsorbent to 300 mL glass vessels and mixing with 100 mL phosphate solution. The pH value of the mixture was adjusted to 6.0 ± 0.1, and the vessels were shaken at 150 rpm for 3 hours at 25 ± 1 °C.

Langmuir and Freundlich isotherms were applied to fit the experimental data. Both linear and nonlinear methods were tested. Mathematical models are listed below.

Langmuir isotherm linear model (Kostura *et al.* 2005):

$$\frac{C_e}{Q_e} = \frac{C_e}{Q_0} + \frac{1}{b}Q_0$$

Langmuir isotherm nonlinear model (Sun *et al.* 2018):

$$q_e = \frac{K_a Q_m C_e}{1 + K_a C_e}$$

Freundlich isotherm linear model (Deliyanni *et al.* 2007):

$$\lg Q_e = \frac{1}{n}\lg C_e + \lg K$$

Freundlich isotherm nonlinear model (Zhang *et al.* 2017):

$$Q_e = K_F C_e^{\frac{1}{n}}$$

where C_e (mg/L) is the solution's concentration of sorbent at equilibrium; b, K_a are the Langmuir linear and nonlinear constants, respectively. K and K_F are the linear and nonlinear Freundlich constants, respectively, n (Freundlich exponent) is an indicator of intensity change during the adsorption process and also an index of deviation from linearity of adsorption. Q_0 and Q_m denote the linear and nonlinear Langmuir maximum capacity (mg/g), respectively. Q_e is phosphate adsorption capacity at equilibrium (mg/g).

Physical characterization

Scanning electron microscopy (SEM) imaging was conducted using a Hitachi S-4800 scanning microscope (Hitachi, Japan) to examine the surface topography of the adsorbent. Specific surface area was determined using a NOVA 2000e analyzer, and Fourier transform infrared spectra (FTIR) were analyzed by an IRPrestige-21 transform infrared spectrometer (Shimadzu, Japan). The data were analyzed using OriginPro 2017.

RESULTS AND DISCUSSION

Effects of heating temperature on phosphate adsorption capacity of CT

Compared with raw CT, thermal modification significantly affected the phosphate adsorption capacity of CT. As the heating temperature increased from 50 °C to 350 °C, the phosphate adsorption capacity of the CT increased significantly. When the temperature exceeded 350 °C, the phosphate adsorption capacity dropped. At 600 °C and 650 °C, the phosphate adsorption capacity was lower than raw CT (Figure 1). The highest adsorption, 3.32 mg/g, was observed in treatments at 310 °C to 350 °C, significantly higher than at other temperatures. No significant differences in capacity were observed when the temperature ranged from 310 °C to 350 °C, suggesting that 310–350 °C might be the best temperature range for thermal modification of CT.

With increasing temperature, CT firstly lost surface and interlayer water, secondly lost bound water from its structural framework, and lastly organic impurities were burned. Therefore, heating modification reduced adsorption resistance derived from water, enhanced porosity and enlarged the surface area of CT, which together improved

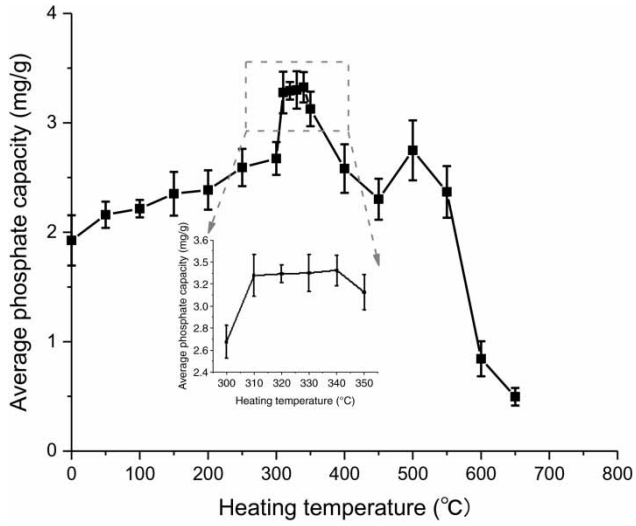

Figure 1 | Effects of heating temperature on phosphate adsorption of copper tailings.

its phosphate adsorption capacity. When the temperature exceeded 600 °C, the structure of adsorbent was destroyed, leading to sintering and stacking, which finally reduced adsorption capacity (Kong *et al.* 2008).

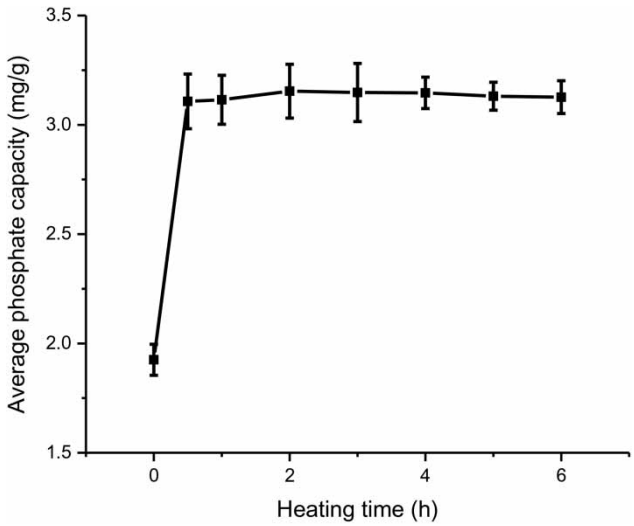

Figure 2 | Effect of heating time on the phosphate adsorption capacity of CT.

Effects of heating time on phosphate adsorption of CT

Effects of heating time on the adsorption ability of CT heated to 350 °C are illustrated in Figure 2. No significant differences in adsorption capacity were observed among treatments with heating times ranging from 0.5 to 6 hours. The highest average value of phosphate adsorption capacity, 3.15 mg/g, was observed from treatment for 2 hours.

Characterization of CT340 and raw CT

SEM images of CT340 and raw CT were compared. Particles of raw CT were relatively larger than CT340, suggesting thermal modification cracked CT. The surface of raw CT particles was relatively smooth, but that of CT340 was rough (Figure 3). These results suggest that the surface area of CT might be enlarged by thermal modification.

The N_2 adsorption-desorption isotherms of raw CT and CT340 and their corresponding Barrett–Joyner–Halenda (BJH) pore size distribution plots are shown in Figure 4. Holes with diameters of less than 2 nm, ranging from 2 nm

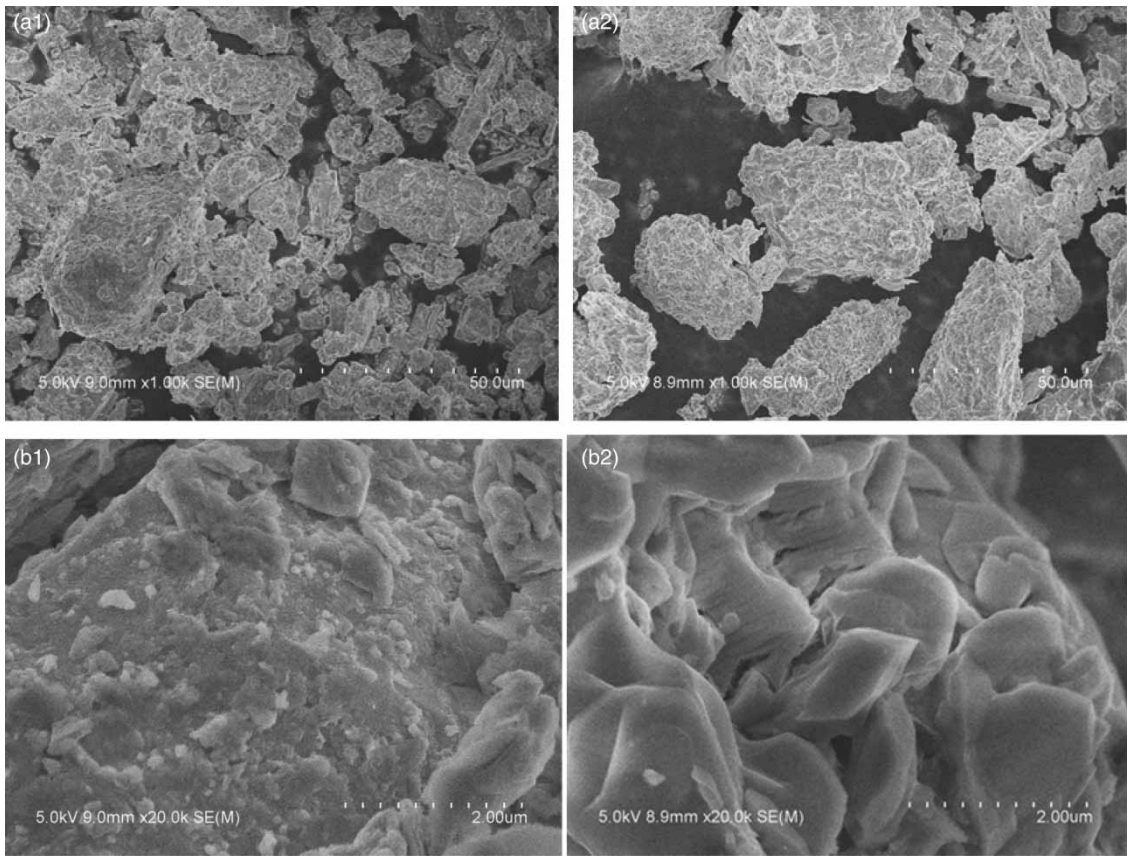

Figure 3 | Scanning electronic microscopy images of copper tailings treated at 340 °C (a_1 and b_1) and raw copper tailings (a_2 and b_2).

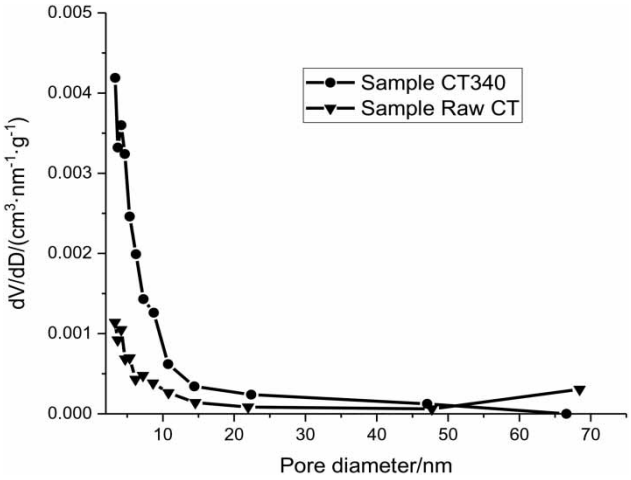

Figure 4 | Pore size–pore volume distribution of raw CT and CT340.

to 50 nm, and greater than 50 nm are called micropores, mesopores (transition pores) and macropores, respectively (Zhang & Wang 2016). Analyses of pore volume pore size distribution showed that pore the size of CT340 and raw CT was mainly 3 nm (mesopore). Moreover, the ratio of mesopores was relatively higher, and that of macropores was lower in CT340 compared with raw CT (Figure 4), demonstrating that the pore size distribution shifted downwards in response to thermal modification.

Heating can increase surface area of products (Evita *et al.* 2013), and enlarged surface area promotes heating rate and reaction time (Schimmelpfenning & Glaser 2012), which further increases the surface area. In the present study, analysis of the surface area showed that the surface area of raw CT and CT340 was 2.994 m^2/g and 6.934 m^2/g, respectively. Clearly, thermal modification noticeably increased the surface area of CT, which should promote phosphate adsorption capacity (San & Tüzen 2013).

FTIR spectra of CT340 and raw CT are shown in Figure 5. The transmittance patterns of CT340 and raw CT are similar, showing peaks at 3,419 cm^{-1}, 1,640 cm^{-1}, 1,110 cm^{-1}, which represent Si-OH stretching vibration, O-H bending vibration and Si-O-Si bending, respectively. Transmittance between 831 cm^{-1} and 433 cm^{-1} was

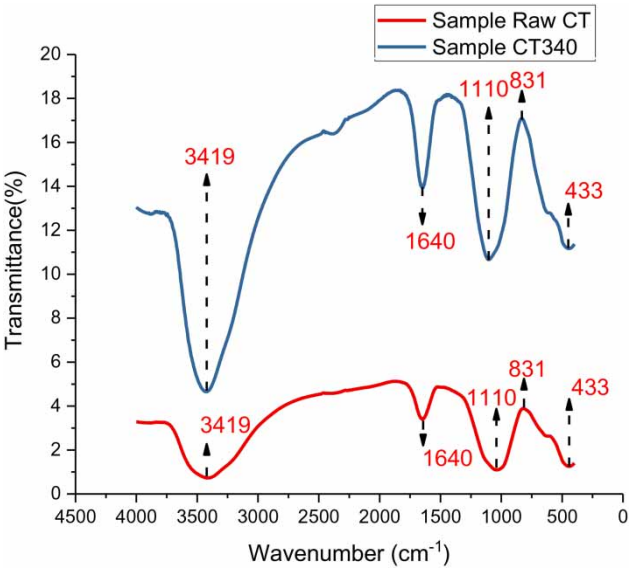

Figure 5 | FTIR spectra of raw CT and CT 340.

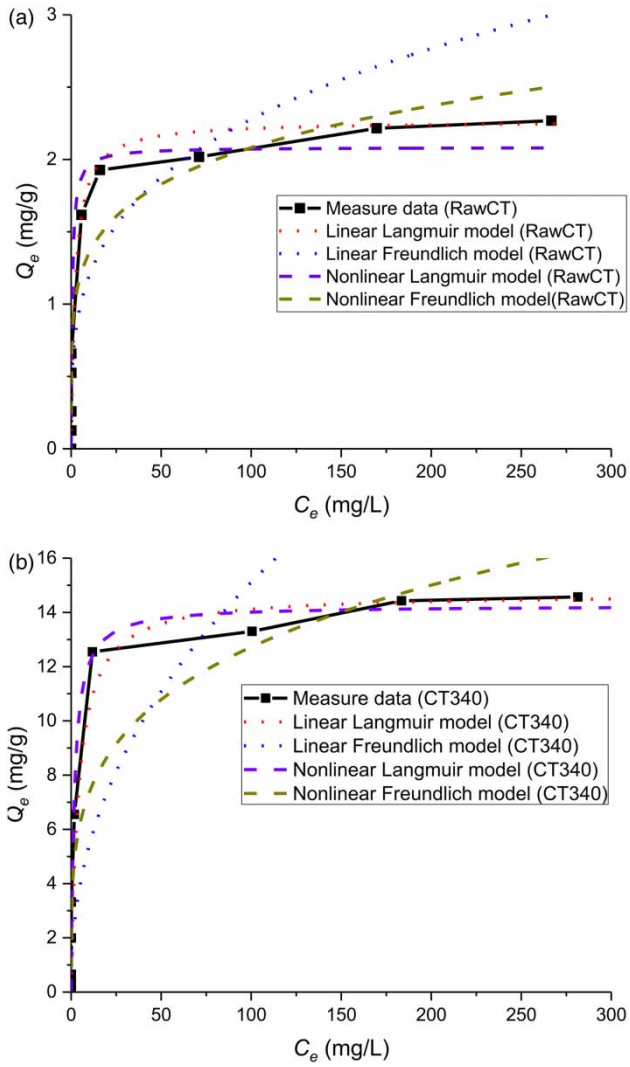

Figure 6 | (a) Adsorption isotherms of phosphate adsorption by raw CT (experimental conditions: dosage of raw copper tailings = 1.5 g; initial phosphate concentration = 0–300 mg/L; temperature = 298 ± 1 K; pH 6.0 ± 0.1). (b) Adsorption isotherms of phosphate adsorption by CT340 (experimental conditions: dosage of raw copper tailings = 1.5 g; initial phosphate concentration = 0–500 mg/L; temperature = 298 ± 1 K; pH6.0 ± 0.1).

Table 1 | Parameters of linear and nonlinear models of Langmuir and Freundlich

			Raw CT	CT340
Linear	Langmuir	K_a	0.427	0.243
		Q_m	2.26	14.69
		R^2	0.9992	0.9982
	Freundlich	K_F	0.6266	1.9302
		1/n	0.2803	0.4468
		R^2	0.7724	0.7214
Nonlinear	Langmuir	K_a	1.57	0.566
		Q_m	2.08	14.25
		R^2	0.9535	0.9802
	Freundlich	K_F	0.1870	4.2509
		1/n	0.8825	0.2380
		R^2	0.8775	0.8749

attributed to the superposition of characteristic vibrations of aluminum and magnesium oxides (Cai *et al.* 2012).

The maximum adsorption capacities of CT340 and raw CT

Adsorption isotherms can be used to predict the maximum adsorption capacity of an adsorbent. Several mathematical formulas have been used to fit experimental data and to evaluate isotherm performance, such as Langmuir, Freundlich, Temkin, Redlich–Peterson, and Sips sorption isotherms (Rostamian *et al.* 2011). Among them, the characteristic feature of the Langmuir isotherm model is monolayer adsorption on a homogeneous surface with a finite number of adsorption sites and without any interaction between adsorbed molecules (Rout *et al.* 2014). The adsorption process of the Freundlich isotherm model is explained when a heterogeneous adsorbent surface is involved in multilayer distribution of adsorbate with interactions between the adsorbed molecules (Rout *et al.* 2014). Since Langmuir and Freundlich isotherms are commonly used (Li *et al.* 2014; Wan *et al.* 2017; Goscianska *et al.* 2018) in similar studies, these two isotherms were applied in the present study.

The fitting results, as summarized in Table 1 and Figure 6, elucidated that all four models showed high R^2, suggesting these models fitted the present experimental data. These results could be interpreted by the complex mineralogical forms present in CT. Moreover, the Langmuir linear and nonlinear models showed better performance than the Freundlich linear and nonlinear models for both raw CT and CT340, since the former had higher R^2. These results indicated that the monolayer adsorption process with intra-molecular interactions might be dominant during phosphate adsorption by CT. Based on the model's prediction, the maximum adsorption capacity of phosphate at 25 °C was 14.25 mg/g for CT340 and 2.08 mg/g for raw CT.

Comparison with other adsorbents

The phosphate adsorption capacity of adsorbents in previous literatures is summarized in Table 2. CT340 showed the highest adsorption capability among all listed adsorbents, which suggested that CT340 might have potential as a phosphate adsorbent for removing phosphate from

Table 2 | Comparison of phosphate adsorption capacity (q_m) among CT340, raw CT with other reported adsorbents

Adsorbents	q_m (mg/g)	pH	Reference
Thermally modified steel slag	13.62	7.0	Yu *et al.* (2015)
Iron oxide tailings	8.21	6.6	Zeng *et al.* (2004)
Mg-Al hydrotalcite-loaded kaolin clay	11.92	7.5	Lin & Zhou (2015)
Acid-modified fly ash	13.3	7.5	Li *et al.* (2016a)
Acid-modified palygorskite	10.5	7.5	Li *et al.* (2016a)
Kanuma clay	4.39	7.0	Yang *et al.* (2013)
Innovative modified bentonites	11.15	7.0	Zamparas *et al.* (2012)
$Ca(OH)_2$-modified natural clinoptilolite	7.57	7.0	Mitrogiannis *et al.* (2017)
Granular boehmite	8.38	7.0	Ogata *et al.* (2012)
Steel byproduct	3.70	7.0	Hua *et al.* (2016)
Raw CT	2.08	6.0	This study
CT340	14.25	6.0	This study

aqueous solutions. However, CT might be harmful to the environment due to high levels of heavy metals. Whether heavy metals could be immobilized by phosphate in real situations and how to avoid environmental contamination with CT should be investigated in future.

CONCLUSION

Copper tailings were heated at different temperatures and for different times, and their phosphate adsorption capability was compared. The results showed that heating temperature had a significant effect but heating time did not influence the phosphate adsorption capacity of thermally modified copper tailings. The optimum temperature ranged from 310 to 350 °C. Thermally modified copper tailings showed higher porosity than raw copper tailings, and the BJH surface area was three times higher than that of raw copper tailings. These characteristics might explain the increased phosphate adsorption ability of copper tailings in response to heating.

ACKNOWLEDGEMENTS

This work was supported by the National Nature Science Foundation of China (No. 51409001), the Excellent Talents Supporting Program of Higher Education of Anhui (No. gxyqZD2016127), the College Natural Science Foundation of Major Project of Anhui, China (KJ2018ZD033), the Foundation of Anhui Provincial Key Laboratory of the Conservation and Exploitation of Biological Resources, and the Center of Analysis and Testing, Anhui Polytechnic University for the SEM, Brunauer–Emmett–Teller (BET), and FTIR analyses. We also express our thanks to reviewers, editors, and Dr Gen Zhang.

REFERENCES

Ashekuzzaman, S. M. & Jiang, J. Q. 2014 Study on the sorption-desorption-regeneration performance of Ca-, Mg- and CaMg-based layered double hydroxides for removing phosphate from water. *Chemical Engineering Journal* **246**, 97–105.

Awual, M. R., Jyo, A., Thara, T., Seko, N., Tamada, M. & Lim, K. T. 2011 Enhanced trace phosphate removal from water by zirconium (IV) loaded fibrous adsorbent. *Water Research* **45** (15), 4592–4600.

Barca, C., Gérente, C., Meyer, D., Chazarenc, F. & Andrés, Y. 2012 Phosphate removal from synthetic and real wastewater using steel slags produced in Europe. *Water Research* **46** (7), 2376–2384.

Bhatnagar, A. & Sillanpää, M. 2010 Utilization of agro-industrial and municipal waste materials as potential adsorbents for water treatment-a review. *Chemical Engineering Journal* **157** (2), 277–296.

Blaney, L. M., Cinar, S. & Sengupta, A. K. 2007 Hybrid anion exchanger for trace phosphate removal from water and waste water. *Water Research* **41** (7), 1603–1613.

Cai, P., Zheng, H., Wang, C., Ma, H. W., Hu, J. C., Pu, Y. B. & Liang, P. 2012 Competitive adsorption characteristic of fluoride and phosphate on calcined Mg-Al-CO_3 layered double hydroxide. *Journal of Hazardous Materials* **213–214** (2), 100–108.

Claveau-Mallet, D., Wallace, S. & Comeau, Y. 2012 Model of phosphorus precipitation and crystal formation in electric arc furnace steel slag filters. *Environmental Science and Technology* **46** (3), 1465–1470.

Cui, X. Q., Dai, X., Khan, K. Y., Li, T. Q., Yang, X. E. & He, Z. L. 2016 Removal of phosphate from aqueous solution using magnesium-alginate/chitosan modified biochar microspheres derived from *Thalia dealbata*. *Bioresource Technology* **218**, 1123–1132.

Dai, J., Yang, H., Yan, H., Shangguan, Y. G., Zheng, Q. & Cheng, R. S. 2011 Phosphate adsorption from aqueous solution by disused adsorbents: chitosan hydrogel beads after the removal of copper (II). *Chemical Engineering Journal* **166** (3), 970–977.

Debashan, L. E. & Bashan, Y. 2004 Recent advances in removing phosphorus from wastewater and its future use as fertilizer (1997–2003). *Water Research* **38** (19), 4222–4246.

Deliyanni, E. A., Peleka, E. N. & Lazaridis, N. K. 2007 Comparative study of phosphates removal from aqueous solutions by nanocrystalline akaganeite and hybrid surfactant-akaganeite. *Separation and Purification Technology* **52** (3), 478–486.

Evita, A., George, B., Dimitrios, K. & Evan, D. 2013 Biochar production by sewage sludge pyrolysis. *Journal of Analytical and Applied Pyrolysis* **101** (5), 72–78.

Franco, D., Lee, J., Arbelaez, S., Cohen, N. & Kim, J. Y. 2017 Removal of phosphate from surface and wastewater via electrocoagulation. *Ecological Engineering* **108**, 589–596.

Gan, L., Lu, Z. Y., Cao, D. & Chen, Z. L. 2018 Effects of cetyltrimethylammonium bromide on the morphology of green synthesized Fe_3O_4 nanoparticles used to remove phosphate. *Materials Science & Engineering C* **82**, 41–45.

Goscianska, J., Koniarz, M. P., Frankowski, M., Franus, M., Panek, R. & Franus, W. 2018 Removal of phosphate from water by lanthanum-modified zeolites obtained from fly ash. *Journal of Colloid and Interface Science* **513**, 72–81.

Hermassi, M., Valderrama, C., Moreno, N., Font, O., Querol, X., Batis, N. H. & Cortina, J. L. 2017 Fly ash as reactive sorbent for phosphate removal from treated waste water as a potential slow release fertilizer. *Journal of Environmental Chemical Engineering* **5** (1), 160–169.

Hua, G. H., Morgan, W. S., Christopher, G. S. & Christopher, H. H. 2016 Nitrate and phosphate removal from agricultural

subsurface drainage using laboratory woodchip bioreactors and recycled steel byproduct filters. *Water Research* **102**, 180–189.

Huang, H. M., Liu, J. H., Zhang, P., Zhang, D. D. & Gao, F. M. 2017 Investigation on the simultaneous removal of fluoride, ammonia nitrogen and phosphate from semiconductor wastewater using chemical precipitation. *Chemical Engineering Journal* **307**, 696–706.

Jiang, F. J., Tan, J., Sun, Q. Y., Li, M. & Wang, W. 2008 Oxidized copper mine tailings and its adsorption on phosphate from aqueous solution. *Environmental Chemistry* **27** (5), 600–604.

Jung, K. W., Hwang, M. J., Jeong, T. U. & Ahn, K. H. 2015 A novel approach for preparation of modified-biochar derived from marine macroalgae: dual purpose electro-modification for improvement of surface area and metal impregnation. *Bioresource Technology* **191** (0), 342–345.

Jung, K. W., Jeong, T. U., Choi, J. W., Ahn, K. H. & Lee, S. H. 2017 Adsorption of phosphate from aqueous solution using electrochemically modified biochar calcium-alginate beads: batch and fixed-bed column performance. *Bioresource Technology* **244** (Pt1), 23–32.

Khan, M. J. & Jones, D. L. 2009 Effect of composts, lime and diammonium phosphate on the phytoavailability of heavy metals in a copper mine tailing soil. *Pedosphere* **19** (5), 631–641.

Kilpimaa, S., Runtti, H., Kangas, T., Lassi, U. & Kuokkanen, T. 2014 Removal of phosphate and nitrate over a modified carbon residue from biomass gasification. *Chemical Engineering Research and Design* **92** (10), 1923–1922.

Koilraj, P. & Sasaki, K. 2017 Selective removal of phosphate using La-porous carbon composites from aqueous solutions: batch and column studies. *Chemical Engineering Journal* **317**, 1059–1068.

Kong, L. Z., Xue, F., Chen, L. L., Sun, Q. Y. & Yang, L. Z. 2008 Adsorption of phosphate on copper mine tailings samples. *Environmental Pollution & Control* **30** (5), 15–18.

Kostura, B., Kulveitova, H. & Lesko, J. 2005 Blast furnace slags as sorbents of phosphate from water solutions. *Water Research* **39** (9), 1795–1802.

Li, G. L., Gao, S., Zhang, G. S. & Zhang, X. W. 2014 Enhanced adsorption of phosphate from aqueous solution by nanostructured iron (III)–copper (II) binary oxides. *Chemical Engineering Journal* **235** (1), 124–131.

Li, F. H., Wu, W. H., Li, R. Y. & Fu, X. R. 2016a Adsorption of phosphate by acid-modified fly ash and palygorskite in aqueous solution: experimental and modeling. *Applied Clay Science* **132–133**, 343–352.

Li, Z. W., Huang, B., Huang, J. Q., Chen, G. Q., Xiong, W. P., Nie, X. D., Ma, W. M. & Zeng, G. M. 2016b Influence of different phosphates on adsorption and leaching of Cu and Zn in red soil. *Transactions of Nonferrous Metals Society of China* **26** (2), 536–543.

Lin, D. & Zhou, S. 2015 Synthesis and characterization of novel Mg-Al hydrotalcite-loaded kaolin clay and its adsorption properties for phosphate in aqueous solution. *Journal of Alloys and Compounds* **637**, 188–196.

Liu, J. Y., Wan, L. H., Zhang, L. & Zhou, Q. 2011 Effect of pH, ionic strength, and temperature on the phosphate adsorption onto lanthanum-doped activated carbon fiber. *Journal of Colloid and Interface Science* **364** (2), 490–496.

Liu, T., Wu, K. & Zeng, L. H. 2012 Removal of phosphorus by a composite metal oxide adsorbent derived from manganese ore tailings. *Journal of Hazardous Materials* **217–218**, 29–35.

Lv, J. B., Liu, H. J., Liu, R. P., Zhao, X., Sun, L. P. & Qu, J. H. 2013 Adsorptive removal of phosphate by a nanostructured Fe-Al-Mn trimetal oxide adsorbent. *Powder Technology* **233** (1), 146–154.

Mignardi, S., Corami, A. & Ferrini, V. 2012 Evaluation of the effectiveness of phosphate treatment for the remediation of mine waste soils contaminated with Cd, Cu, Pb, and Zn. *Chemosphere* **86** (4), 354–360.

Mitrogiannis, D., Psychoyou, M., Baziotis, I., Inglezakis, V. J., Koukouzas, N., Tsoukalas, N., Palles, D., Kamitsos, E., Oikonomou, G. & Markou, G. 2017 Removal of phosphate from aqueous solutions by adsorption onto $Ca(OH)_2$ treated natural clinoptilolite. *Chemical Engineering Journal* **320**, 510–522.

Mouiya, M., Abourriche, A., Bouazizi, A., Benhammou, A., Hafiane, Y. E., Abouliatim, Y., Nibou, L., Oumam, M., Ouammou, M., Smith, A. & Hannache, H. 2018 Flat ceramic microfiltration membrane based on natural clay and Moroccan phosphate for desalination and industrial wastewater treatment. *Desalination* **427**, 42–50.

Ogata, F., Tominaga, H., Kangawa, M., Inoue, K. & Kawasaki, N. 2012 Characteristics of granular boehmite and its ability to adsorb phosphate from aqueous solution. *Chemical and Pharmaceutical Bulletin (Tokyo)* **60** (8), 985–988.

Park, J. H., Ok, Y. S., Kim, S. H., Cho, J. S., Heo, J. S., Delaune, R. D. & Seo, D. C. 2015 Evaluation of phosphorus phosphate adsorption capacity of sesame straw biochar on aqueous solution: influence of activation methods and pyrolysis temperature. *Environmental Geochemistry & Health* **37** (6), 969–983.

Park, T., Ampunan, V., Maeng, S. & Chung, E. 2017 Application of steel slag coated with sodium hydroxide to enhance precipitation-coagulation for phosphorus removal. *Chemosphere* **167**, 91–97.

Ren, J., Li, N., Li, L., An, J. K., Zhao, L. & Ren, N. Q. 2015a Granulation and ferric oxides loading enable biochar derived from cotton stalk to remove phosphate from water. *Bioresource Technology* **178**, 119–125.

Ren, X., Tan, X., Hayat, T., Alsaedi, A. & Wang, X. 2015b Co-sequestration of Zn (II) and phosphate by gamma-al_2o_3: from macroscopic to microscopic investigation. *Journal of Hazardous Materials* **297**, 134–145.

Rostamian, R., Najafi, M. & Rafati, A. A. 2011 Synthesis characterization of thiol-functionalized silica nano hollow sphere as a novel adsorbent for removal of poisonous heavy metal ions from water: kinetics, isotherms and error analysis. *Chemical Engineering Journal* **171** (3), 1004–1011.

Rout, P. R., Bhunia, P. & Dash, R. R. 2014 Modeling isotherms, Kinetics and understanding the mechanism of phosphate

adsorption onto a solid waste: ground burnt patties. *Journal of Environment Chemical Engineering* **2** (3), 1331–1342.

San, A. & Tüzen, M. 2013 Adsorption of silver from aqueous solution onto raw vermiculite and manganese oxide-modified vermiculite. *Microporous and Mesoporous Materials* **170** (170), 155–163.

Schimmelpfenning, S. & Glaser, B. 2012 One step forward toward characterization: some important material properties to distinguish biochars. *Journal of Environmental Quality* **41** (4), 1001–1013.

Sevcenco, A. M., Paravidino, M., Vrouwenvelder, J. S., Wolterbeek, H. T., Loosdrecht, M. C. M. V. & Hagen, W. R. 2015 Phosphate and arsenate removal efficiency by thermostable ferritin enzyme from *Pyrococcus furiosus* using radioisotopes. *Water Research* **76**, 181–186.

Song, L. Z., Huo, J. B., Wang, X. L., Yang, F. F., He, J. & Li, C. Y. 2016 Phosphate adsorption by a Cu(II)-loaded polyethersulfone-type metal affinity membrane with the presence of coexistent ions. *Chemical Engineering Journal* **284**, 182–193.

Sun, Z. H., Chen, D. Y., Chen, B. D., Kong, L. J. & Su, M. H. 2018 Enhanced uranium(VI) adsorption by chitosan modified phosphate rock. *Colloids and Surfaces A: Physicochemical and Engineering Aspects*. https://doi.org/10.1016/j.colsurfa.2018.02.043.

Van Voorthuizen, E. M., Zwijnenburg, A. & Wessling, M. 2005 Nutrient removal by NF and RO membranes in a decentralized sanitation system. *Water Research* **39** (15), 3657–3667.

Wan, S. F., Wang, S. S., Li, Y. C. & Gao, B. 2017 Functionalizing biochar with Mg–Al and Mg–Fe layered double hydroxides for removal of phosphate from aqueous solutions. *Journal of Industrial and Engineering Chemistry* **47**, 246–253.

Wang, Y., Yu, Y. G., Li, H. Y. & Shen, C. C. 2016a Comparison study of phosphorus adsorption on different waste solids: fly ash, red mud and ferric–alum water treatment residues. *Journal of Environmental Sciences* **50** (12), 79–86.

Wang, Z. H., Shen, D. K., Shen, F. & Li, T. Y. 2016b Phosphate adsorption on lanthanum loaded biochar. *Chemosphere* **150**, 1–7.

Wei, F. S. & Qi, W. Q. 2009 *Monitoring Method for Water and Waste Water (Fourth Edition)*. PRC Ministry of Environmental Protection, Peking, P.R. China, pp. 246–247.

Xu, K., Deng, T., Liu, J. T. & Peng, W. G. 2010 Study on the phosphate removal from aqueous solution using modified fly ash. *Fuel* **89** (12), 3668–3674.

Yang, S. J., Zhao, Y. X., Chen, R. Z., Feng, C. P., Zhang, Z. Y., Lei, Z. F. & Yang, Y. N. 2013 A novel tablet porous material developed as adsorbent for phosphate removal and recycling. *Journal of Colloid and Interface Science* **396** (6), 197–204.

Yang, Q., Wang, X. L., Luo, W., Sun, J., Xu, Q. X., Chen, F., Zhao, J. W., Wang, S. N., Yao, F. B., Wang, D. B., Li, X. M. & Zeng, G. M. 2018 Effectiveness and mechanisms of phosphate adsorption on iron-modified biochars derived from waste activated sludge. *Bioresource Technology* **247**, 537–544.

Ye, J., Cong, X. N., Zhang, P. Y., Zeng, G. M., Hoffmann, E., Wu, Y., Zhang, H. B. & Fang, W. 2016 Operational parameter impact and back propagation artificial neural network modeling for phosphate adsorption onto acid-activated neutralized red mud. *Journal of Molecular Liquids* **216**, 35–41.

Yu, J., Liang, W. Y., Wang, L., Li, F. Z., Zou, Y. L. & Wang, H. D. 2015 Phosphate removal from domestic wastewater using thermally modified steel slag. *Journal of Environmental Sciences* **31** (5), 81–88.

Zamparas, M., Gianni, A., Stathis, P., Deligiannakis, Y. & Zacharias, I. 2012 Removal of phosphate from natural waters using innovative modified bentonites. *Applied Clay Science* **62–63** (7), 101–106.

Zeng, L., Li, X. M. & Liu, J. D. 2004 Adsorptive removal of phosphate from aqueous solutions using iron oxide tailings. *Water Research* **38** (5), 1318–1326.

Zhang, X. X. & Wang, X. 2016 Study of the preparation of *Salix psammophila* activated carbons by the activation of H_3PO_4. *Journal of Forestry Engineering* **1**, 58–62.

Zhang, H., Chen, Z., Gao, Y. & Sun, Q. Y. 2010 Adsorption-desorption characteristics of dissolved phosphorus on surface of copper mine tailings. *Journal of Agro-Environment Science* **29** (8), 1542–1546.

Zhang, J. D., Shen, Z. M., Mei, Z. J., Li, S. P. & Wang, W. H. 2011a Removal of phosphate by Fe-coordinated amino-functionalized 3D mesoporous silicates hybrid materials. *Journal of Environmental Sciences* **23** (2), 199–205.

Zhang, J. D., Shen, Z. M., Shan, W. P., Mei, Z. J. & Wang, W. H. 2011b Adsorption behavior of phosphate on lanthanum (III) – coordinated diamino-functionalized 3D hybrid mesoporous silicates materials. *Journal of Hazardous Materials* **186** (1), 76–83.

Zhang, C., Li, Y. Q., Wang, F. H., Yu, Z. G., Wei, J. J., Yang, Z. Z., Ma, C., Li, Z. H., Xu, Z. Y. & Zeng, G. M. 2017 Performance of magnetic zirconium-iron oxide nanoparticle in the removal of phosphate from aqueous solution. *Applied Surface Science* **396**, 1783–1792.

Zhao, Y., Zhang, L. Y., Ni, .F., Xi, B. D., Xia, X. F., Peng, X. J. & Luan, Z. K. 2011 Evaluation of a novel composite inorganic coagulant prepared by red mud for phosphate removal. *Desalination* **273** (2), 414–420.

First received 13 December 2017; accepted in revised form 9 May 2018. Available online 18 May 2018